

Viable Circulating Tumor Cell Enrichment by Flexible Micro Spring Array

Ramdane A. Harouaka, Ming-Da Zhou, Tim Y. Yeh, Waleed J. Khan, Jeffery Allerton and Si-Yang Zheng *Member, IEEE*

Abstract— We demonstrated a high throughput versatile platform capable of isolating circulating tumor cells (CTCs) from clinically relevant volumes of blood while preserving their viability and ability to proliferate. The enrichment is based on the fact that CTCs are larger compared with normal blood cells. The incorporated system allows size-based separation of CTCs at the micro-scale, while taking advantage of a high throughput and rapid processing speed. Testing results of model systems using cell lines show that this device can enrich CTCs from 7.5 mL of whole blood samples with 90% capture efficiency, higher than 10^4 enrichment, and better than 80% viability in approximately ten minutes without any incidence of clogging.

I. INTRODUCTION

According to WHO projections cancer is now the leading cause of mortality worldwide, representing 1 out of every 8 fatalities [1]. The ability of metastatic cancer to release cells that travel through the circulatory system and invade different parts of the body accounts for over 90% of cancer related deaths [2]. Despite its importance, some key processes during metastasis are still elusive and effective approaches to cure metastatic diseases are largely unavailable. Part of the challenge is the lack of technology to study and diagnose metastasis on an individual patient basis at a molecular level. During metastasis, malignant circulating tumor cells (CTCs) detach from the primary tumor, spread through peripheral blood, then invade and proliferate in distant organs. Analysis of CTCs will allow the prognosis and evaluation of therapies as they relate directly to metastases [3].

CTCs are rare in blood on the order of one out of a billion blood cells [4-6]. These epithelial cells are larger and stiffer than normal blood cells. Size-base enrichment is a cost-effective way based on intrinsic physical parameters (size and deformability). It doesn't require the knowledge of molecular markers on cell surface, thus it is independent of cell surface antigen expression level and cell labeling is not needed. The corresponding author and his collaborators designed the first microfabricated filter for CTC enrichment before [7, 8]. Similar to conventional pore-shaped track-etched filters, it can't maintain the viability of enriched cells. Further investigation of complicated 3D microfiltration structures demonstrated the feasibility of viable CTC enrichment but

devices are limited by the processable sample volume within 1 mL range [9]. In this paper, we report a new device, the flexible micro spring array (FMSA) device, which enables viable CTC enrichment of clinic relevant blood volume.

II. DEVICE DESIGN AND FABRICATION

The FMSA device incorporates new design principles for size-exclusion based microfiltration device: (1) By implementing 2D flexible polymer microsprings as an effective microfiltration structure, it compensates for the mechanical properties of tumor cells while making the fabrication process straightforward for excellent yield; (2) By maximizing device porosity, it increases sample capacity for a given device surface area to prevent clogging; (3) By applying a pressure regulation system to drive the enrichment at extremely low differential pressure, it minimizes the mechanical stress and damage experienced by cells during enrichment to keep them viable.

A. FMSA Device Design

The FMSA device is a single layer of patterned parylene membrane with overall surface area of 1 cm by 1 cm and thickness of 10 μm . Each device has 4 FMSA patches and each patch is a 10x10 array of microspring structures (Figure 1). During enrichment cells go into the plane while larger cells are captured by the microspring structures.

B. Device Simulation

The FMSA device has flexible spring structures capable of deformation in response to applied stress. The stiffness of the microspring structures can be controlled by the parylene width w , the parylene thickness h , the spring width d and the number of anchor pairs n . Finite element analysis was carried out to study the effects of these geometric parameters on device flexibility (Figure 2). A whole patch with four rows of microsprings was modeled, representing an entire functional unit of the device. Each row consisted of a spring with fourteen and a half turns. Boundary conditions were applied to the surface of the anchors that connect the microsprings to the frame and all six degrees of freedom were restricted. The Young's modulus and Poisson's ratio of the parylene microspring material were set to be 2.76 GPa and 0.4, respectively [10, 11]. Without knowing the optimal working pressure at the time of the simulation, a uniform pressure of 0.1 pounds per square inch (psi) equivalently 2.77 inch WC was applied to the top surface of the microspring. The maximal out-of-plane deformation was calculated in post-processing. Each of the four geometric parameters was studied independently while keeping the other three at the

R. A. Harouaka, M.-D. Zhou, T. Y. Yeh, W. J. Khan, and S.-Y. Zheng are with Micro & Nano Integrated Biosystems (MINIBio) Laboratory, Department of Bioengineering and Material Research Institute, The Pennsylvania State University, University Park, PA 16802 USA (corresponding author: 814-865-8090; fax: 814-863-0490; e-mail: siyang@psu.edu).

Jeffery Allerton is with Penn State Hershey Medical Group Benner Pike, State College, PA 16801 USA.

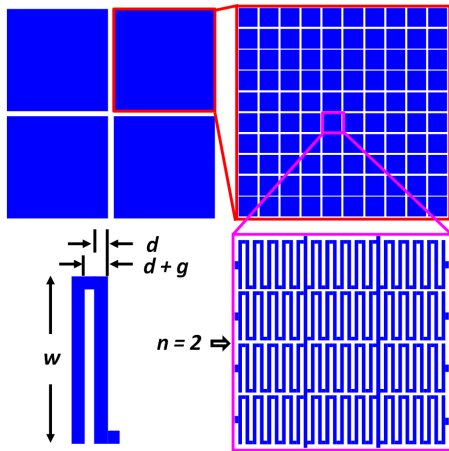


Figure 1. FMSA device design showing top view and important geometrical parameters.

final design values (labeled as red circles in Figure 2B). First, we examined the influence of the parylene thickness h on the out-of-plane deformation of the microspring structures. As the parylene thickness increases from 6 to 20 μm , the deformation decreases dramatically from 10.7 to 0.6 μm . Thus the parylene thickness is a parameter that can be used to

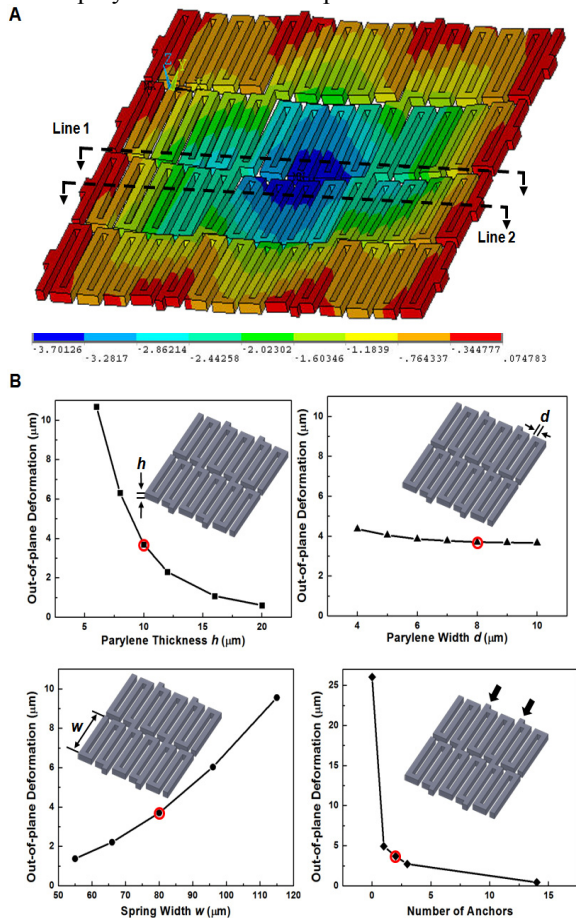


Figure 2. Finite element simulation on the flexibility of the FMSA structure. A: Color coded out-of-plane displacement of a microspring patch under 0.1 psi pressure. B: Geometric effects (parylene thickness, parylene width, spring width and number of anchors) on the maximal out-of-plane deformation. Red circles denote the geometric parameters used in final device fabrication and characterization.

significantly change the flexibility of the microspring structures during fabrication for a given mask design. Next, the influence of parylene width d was examined, while keeping the periodicity $d + g$ as a constant. The maximal out-of-plane deformation decreases slightly as the parylene width increases. This is the least influential of the four geometric parameters we examined. The simulation results of changing spring width w shows the maximal out-of-plane deformation increases as the spring width increases. Finally the effect of the number of additional anchors to the frame was studied and showed that even adding a single anchor can greatly stabilize the microspring structures.

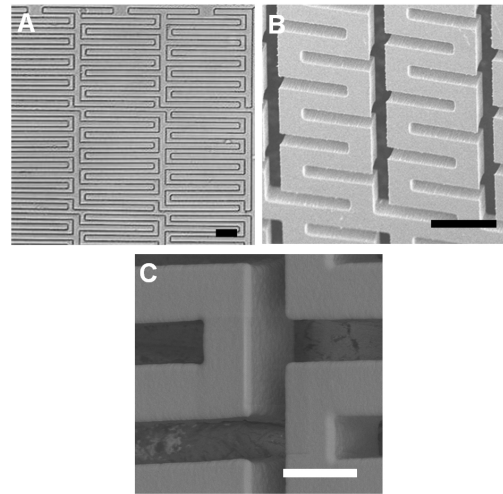


Figure 3. Fabricated FMSA device. A: bright field optical microscopic image of an area of a standard FMSA device. B: SEM image of a FMSA device with shorter spring width. C: SEM image of a FMSA device after refill. Scale bars for A and B are 30 μm . Scale bar for C is 10 μm .

C. Device Fabrication

The device is fabricated on a 10 μm -thick parylene membrane (Figure 3) and the gaps between microsprings are the effective filtration geometry. The microfabrication process was reported before [8]. Briefly, 10 μm -thick parylene was deposited on prime silicon wafer with a room temperature CVD process, and then patterned by photolithography using metal as mask and oxygen plasma dry etching (Figure 3A). The sidewall of the parylene can be well controlled to be vertical (85-90 degree to surface as shown in Figure 3B). After the devices are released from silicon wafer, further parylene deposition (refill) and annealing can reduce the gap width to an ideal value (Figure 3C). The conformal coating guarantees the geometry of the microspring structure is unchanged.

D. Device Testing System

The FMSA device is assembled in a custom-made holder and driven by precise regulated low differential pressure. A simple, disposable vacuum chamber was constructed with a standard 50 mL centrifuge tube with a molded stopper. Pressure measurements were taken with a commercial MEMS pressure sensor that has a sensing range of 0 to ± 10 inch WC, response time of 8 ms and accuracy of $\pm 2.5\%$. Its small footprint allows it to be placed very close to the actual

device. A fine mechanical needle valve was used to manually set the desired filtration pressure. A typical shop vacuum line or alternatively the vacuum connection inside a tissue culture hood was used as the source for vacuum suction. In general, a flow rate of ~ 0.7 mL/min was maintained during enrichment.

III. RESULTS AND DISCUSSION

The performance of the FMSA device was first tested with a model system of cultured cell lines spiked in healthy donor blood. After the concept was validated and the system optimized, clinic samples were demonstrated.

A. Measurement of CTC Capture Efficiency and Enrichment Relative to Leukocytes

We measured the capture efficiency and enrichment of the FMSA device by using four common metastatic carcinoma cell lines (breast cancer cells MCF-7, MDA-MB231; melanoma cells C8161, WM35) spiked in peripheral blood collected from healthy donors. The tumor cells are either green fluorescence labeled with intrinsic GFP expression or fluorescence labeled with chemical dyes before spiking. The capture efficiency and enrichment relative to leukocytes are functions of gap width (Figure 4). When gap width is small (e.g. 4 mm), capture efficiency of 94% can be achieved. In general the device has an enrichment of 104 relative to leukocytes. Both capture efficiency and enrichment are better or similar to previous rigid pore-shaped microfiltration devices for CTC applications [8, 12].

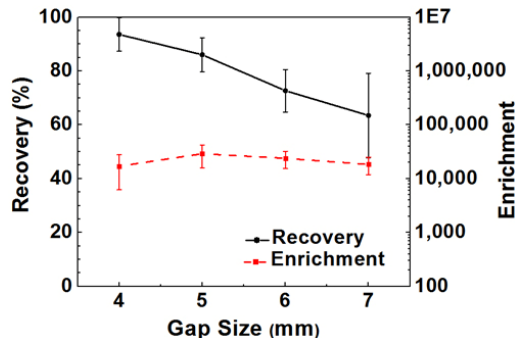


Figure 4. Optimization for capture efficiency and enrichment. Capture efficiency and enrichment under various gap widths are measured and plotted. Each point represent an average and standard deviation of at least 12 data points.

B. Effect and Anticoagulants and Blood Sample Freshness

The type of anticoagulant and freshness of blood sample affect the maximal processable blood volume (Figure 5). Since CTCs are expected to be in much smaller numbers compared with large leukocytes that are captured by the device, the maximal processable blood volume is determined by the number and size distribution of leukocytes. We used blood samples without tumor cell spiking for this part of the investigation. For fresh blood within four hours of withdrawal, 7.5 mL blood in an EDTA tube can be processed using the device with driving a pressure under 0.1 inch WC. 6.5 mL of both fresh and one day old blood in sodium citrate tubes can easily flow through the device without even noticeable positive pressure. 0.5 inch WC pressure is needed

to process 7.5 mL of one day old blood in an EDTA tube, which is a significant pressure increment. We found even fresh blood in lithium heparin tube requires 0.5 inch WC pressure to process 7.5 mL of blood. Although the required driving pressures have no significant difference between one day old sample and fresh sample in lithium heparin tubes, the filter area wrinkles severely with the one day old lithium heparin blood, which does not happen for all the other cases. We processed over 100 fresh blood samples using EDTA as anticoagulant from healthy donors and patients without a single incidence of clogging.

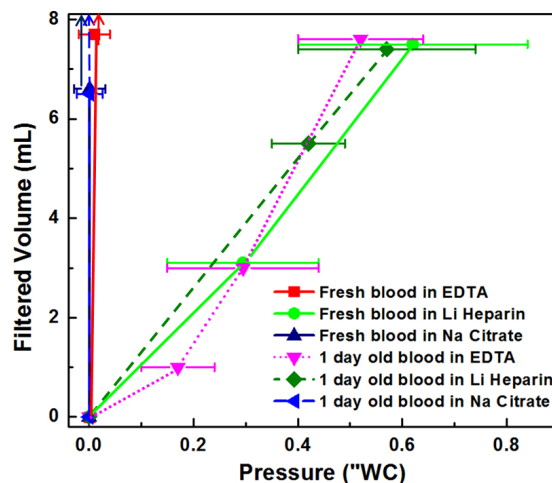


Figure 5. Effect of freshness and anticoagulant type on processable blood volume. For the cases of sodium citrate as the anticoagulant and fresh blood in EDTA (labeled with upward arrows), the driving pressures were so low and the tested blood volumes are expected to be lower than the maximal volumes that can be processed. The rest of the data points represent the maximal blood volumes that can be processed under the specified pressure.

C. Cell Viability and Proliferability

The FMSA requires a differential pressure to drive whole blood samples through the device. The cell viability and proliferability are highly dependent on the driving pressure and the requirement of extremely low driving pressure explains the failure of previous similar viable enrichment efforts. In Figure 6A, a small number of MDA-MB231 cells (<50) pre-labeled with green fluorescent viable cell indicator Calcein-AM (10 μ M) were spiked into 0.5 mL of peripheral blood and filtered through the FMSA device at driving pressures of 1"WC, 5"WC and 10"WC, and then stained with red fluorescent exclusion dye Ethidium Homodimer-1 (4 μ M). Keeping low driving pressure in the range of 1-2"WC is critical for cell viability. In Figure 6B, ~ 130 MCF-7 cells were spiked in 0.5 mL of peripheral blood and enriched under two driving pressures: low pressure (<3"WC) and unregulated pressure with gentle thumb push on the syringe plunger. After 5 days, 40 and 15 colonies were recovered with the two cases respectively. The difference between cell viability and proliferability can be explained by the fact that viability is a short time measurement while proliferability is an evaluation of a longer term effect. Excessive driving pressures during enrichment may have a negative effect on proliferability without any immediately measurable difference in viability [13]. The cell viability is further demonstrated by following colony expansion from 10 labeled

single cells spiked in 1mL whole blood and enriched by FMSA (Figure 6).

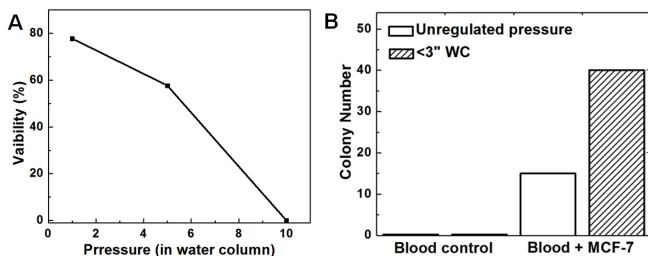


Figure 6. Effect of driving pressure on cell viability. A: Effect of pressure on cell viability on device of 5 μm gap width. B: Effect of pressure on cell proliferation after enrichment.

D. Clinical CTC Enrichment and Detection

Although the FMSA device is designed for viable CTC enrichment and CTC analysis that might depend on cell viability and proliferability afterwards, it can be used as a high performance CTC enumeration device similar to previous CTC microfilters [7-9]. It has the advantage that blood does not need to be partially fixed. After the same viable enrichment procedure, immunocytochemistry (ICC) was used for CTC detection directly on device and Pan-CK+/CD45-/DAPI+ cells are identified as CTCs. Figure 7 shows both single CTCs and a CTC cluster can be identified from a metastatic patient sample (73 year old male, lung cancer small cell, stage IV).

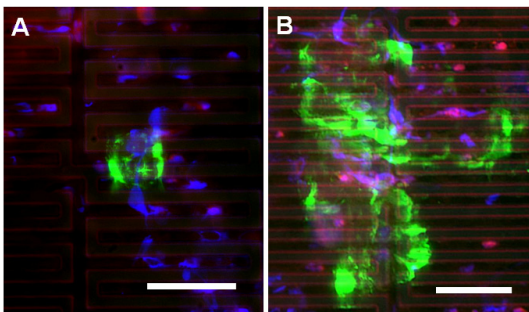


Figure 7. Immunocytochemical detection of CTCs from a 73 year old male diagnosed with Stage IV Small Cell Lung Carcinoma: pan-CK (green), CD45 (red) and PI (blue). A: A single CTC from a clinical sample. B: A cluster of CTCs from the same clinical sample. Scale bars are 50 μm .

IV. CONCLUSION

The FMSA device enables microfiltration to enrich extremely rare CTCs and maintain their viability with clinical relevant blood volume, which has never been achieved before to the best knowledge of the authors. It provides a crucial alternative to popular immunological CTC enrichment which is limited by the expression of specific cell surface markers. Further development may allow an attractive personalized therapeutic strategy for metastatic cancers in which CTCs are genetically analyzed and culture for drug sensitivity test *ex vivo* before the patient goes into expensive, length and painful chemotherapy. The technology can be extended for other size-based cell enrichment applications.

ACKNOWLEDGMENT

The authors appreciate assistance and help from the Penn State Material Research Institute (MRI) and Nanofabrication Laboratory (Nanofab). We would also like to express our thanks to Mr. Gene Gerber, advanced engineering staff of the Bioengineering department, for his help with device characterization; Dr. Philip A Lowry, former oncologist at the Mount Nittany Physician Group, for his encouraging discussion at the beginning of the study; and staff at the Clinical and Translational Science Institute (CTSI) of the Pennsylvania State University, for their help of collecting blood from healthy donors. Melanoma cell lines WM35 and GFP labeled C8161 were generously provided by Dr. Cheng Dong at the Pennsylvania State University. Breast cancer cell lines MCF-7 and MDA-MB231 were obtained from Dr. Henry Lin at the Oak Ridge National Lab.

REFERENCES

- [1] P. Boyle and B. Levin, Eds., *IARC World cancer report*. WHO, 2008.
- [2] P. Mehlen and A. Puisieux, "Metastasis: a question of life or death," *Nat Rev Cancer*, vol. 6, pp. 449-458, 2006.
- [3] M. Cristofanilli, G. T. Budd, M. J. Ellis, A. Stopeck, J. Matera, M. C. Miller, J. M. Reuben, G. V. Doyle, W. J. Allard, L. W. M. M. Terstappen, and D. F. Hayes, "Circulating Tumor Cells, Disease Progression, and Survival in Metastatic Breast Cancer," *N Engl J Med*, vol. 351, pp. 781-791, August 19, 2004 2004.
- [4] P. S. Steeg, "Tumor metastasis: mechanistic insights and clinical challenges," *Nature Medicine*, vol. 12, pp. 895-904, Aug 2006.
- [5] K. Pantel and R. H. Brakenhoff, "Dissecting the metastatic cascade," *Nature Reviews Cancer*, vol. 4, pp. 448-456, Jun 2004.
- [6] K. Pantel, R. H. Brakenhoff, and B. Brandt, "Detection, clinical relevance and specific biological properties of disseminating tumour cells," *Nature Reviews Cancer*, vol. 8, pp. 329-340, May 2008.
- [7] H. K. Lin, S. Zheng, A. J. Williams, M. Balic, S. Groshen, H. I. Scher, M. Fleisher, W. Stadler, R. H. Datar, Y. C. Tai, and R. J. Cote, "Portable filter-based microdevice for detection and characterization of circulating tumor cells," *Clin Cancer Res*, vol. 16, pp. 5011-5018, 2010.
- [8] S. Zheng, H. K. Lin, J.-Q. Liu, M. Balic, R. Datar, R. J. Cote, and Y.-C. Tai, "Membrane microfilter device for selective capture, electrolysis and genomic analysis of human circulating tumor cells," *Journal of Chromatography A*, vol. 1162, pp. 154-161, 2007.
- [9] S. Zheng, H. K. Lin, B. Lu, A. Williams, R. H. Datar, R. J. Cote, and Y. C. Tai, "3D Microfilter Device for Viable Circulating Tumor Cell (CTC) Enrichment from Blood," *Biomedical Microdevices*, vol. 13, p. 203, 2011.
- [10] *SCS parylene properties*. Available: Specialty Coating Systems, Inc. (2007).
- [11] C. Shih, T. Harder, and Y. Tai, "Yield strength of thin-film parylene-C," *Microsystem Technologies*, vol. 10, pp. 407-411, 2004.
- [12] G. Vona, A. Sabile, M. Louha, V. Sitruk, S. Romana, K. Schutze, F. Capron, D. Franco, M. Pazzagli, M. Vekemans, B. Lacour, C. Brechot, and P. Paterlini-Brechot, "Isolation by size of epithelial tumor cells - A new method for the immunomorphological and molecular characterization of circulating tumor cells," *American Journal Of Pathology*, vol. 156, pp. 57-63, Jan 2000.
- [13] J. Hua, L. E. Erickson, T.-Y. Yiin, and L. A. Glasgow, "A Review of the Effects of Shear and Interfacial Phenomena on Cell Viability," *Critical Reviews in Biotechnology*, vol. 13, pp. 305-328, 1993.